ISSN 2618-1584 Vol. 6, Issue 2: 98-107, DOI: 10.25236/FMSR.2024.060215

Exploring the mechanism of action of artesunate against non-small cell lung cancer based on network pharmacology and molecular docking

Liu Qi[1,a], Shen Faqian[1,b], Ma Hu[2,c,*]

[1]*Zunyi Medical University, Zunyi, Guizhou, 563000, China*
[2]*Department of Thoracic Oncology, The Second Affiliated Hospital of Zunyi Medical University, Zunyi, Guizhou, 563000, China*
[a]*liuqi427999@163.com,* [b]*shenfq1213@163.com,* [c]*mahuab@163.com*
[*]*Corresponding author*

Abstract: *The potential targets and pathways of action of artesunate against non-small cell lung cancer were investigated in this study. The two-dimensional chemical structure of artesunate was determined using Pubchem. Several databases, including Swiss Target Prediction, Pharm Mapper, Gene Cards, and OMIM, were used to identify the targets for artesunate and non-small cell lung cancer. Venny online software was used to identify the shared targets between the two drugs, while the STRING database provided the protein-protein interaction network. A "drug component-target-disease" network was created using Cytoscape software. Through the analysis of the OMIM databases, 3280 non-small cell lung cancer disease targets were identified. The potential effects of artesunate against non-small cell lung cancer were determined by finding the intersection of the targets for artesunate and non-small cell lung cancer. GO enrichment analysis using David's database revealed common targets and identified 46 biological pathways that were affected. Further analysis using the Kyoto Encyclopedia of Genes and Genomes (KEGG) identified 81 major pathways. The study also conducted molecular docking studies of six important molecules with artesunate, and it was found that all of them displayed strong binding activity. This information suggests that artesunate may have a significant impact on non-small cell lung cancer through its interaction with these key targets. In conclusion, the use of network pharmacology and molecular docking allowed for the prediction of the target and signaling pathway of artesunate against non-small cell lung cancer. These findings provide a scientific basis for further investigation into the anti-non-small cell lung cancer actions of artesunate.*

Keywords: *Artesunate; Non-small Cell Lung Cancer; Network Pharmacology; Molecular Docking*

1. Introduction

Lung cancer is the leading cause of cancer-related deaths worldwide[1]. According to the latest estimated cancer burden data for 2022, China has twice as many new cases of the disease as the United States, but it also has around five times as many deaths. The most frequent cancer in China is still lung cancer, which also kills more people from the disease in China and the US[2]. According to the pathological type, lung cancer is typically divided into small cell lung cancer (SCLC) and non-small cell lung cancer (NSCLC),of which NSCLC accounts for about 85% of lung cancer[3, 4]. Although surgical resection, radiotherapy, chemotherapy, targeted therapy, immunotherapy, and other techniques continue to be developed, the overall cure and survival rates of NSCLC remain low, especially for advanced metastatic disease[5]. Consequently, to increase the clinical benefit and enhance the treatment result of NSCLC, ongoing research on new targeted medicines and combination therapies is required. A growing number of biological, chemical, and clinical studies and clinical trials have provided scientific evidence for the use of Chinese medicine in the treatment of cancer, which is also gradually being recognized globally as a complementary and alternative therapy for cancer. Chinese medicine exerts its antitumor effects through multiple pathways as a result of its multi-component and multi-target characteristics.

Artesunate (ART), also known as artesunate, with molecular formula $C_{19}O_8H_{28}$, is obtained by esterification of dihydroartemisinin and succinic anhydride, and has pharmacological effects such as antimalarial, antiviral, anti-inflammatory, antitumor and immunomodulatory, and is highly effective, fast-acting, less toxic, and less prone to drug resistance[6]. Inhibition of tumor cell proliferation, induction of apoptosis and cell cycle arrest[7], mitigation of drug resistance[8], inhibition of cancer cell

ISSN 2618-1584 Vol. 6, Issue 2: 98-107, DOI: 10.25236/FMSR.2024.060215

invasion, metastasis, and angiogenesis[9], and regulation of immune cytokine secretion are just a few of the positive effects of ART in different cancers that have been recently discovered[10]. Even though a number of tumor-related signaling pathways, including the PI3K/AKT/FKHR, MAPK, and NF-κB signaling pathways [11-13], have been reported in ART-mediated cancer therapy, the potential molecular mechanisms of artesunate action in cancer, particularly non-small cell lung cancer, are still poorly understood and need further research to inform clinical applications. However, the potential molecular pathways of artesunate in cancer, notably in non-small cell lung cancer, are yet fully understood and need to be further explored to guide therapeutic applications.

An important way for finding new drug targets is network pharmacology, which blends systems biology and network theories[14]. Using high-throughput screening and analytics, it also aids in the development of predictive "drug-targeted illness" network models. By modelling the interaction pattern between receptors and medicines, molecular docking is a technique for creating new medications. The use of molecular docking to describe the mechanism of action has developed into a trend in the development of novel drugs in recent years. In this study, we used molecular docking and network pharmacology to unravel the probable molecular mechanisms of ART in NSCLC, disclose the potential shared targets between ART and NSCLC, and provide further references for artesunate research against NSCLC. All procedures used in this report are shown in Figure 1.

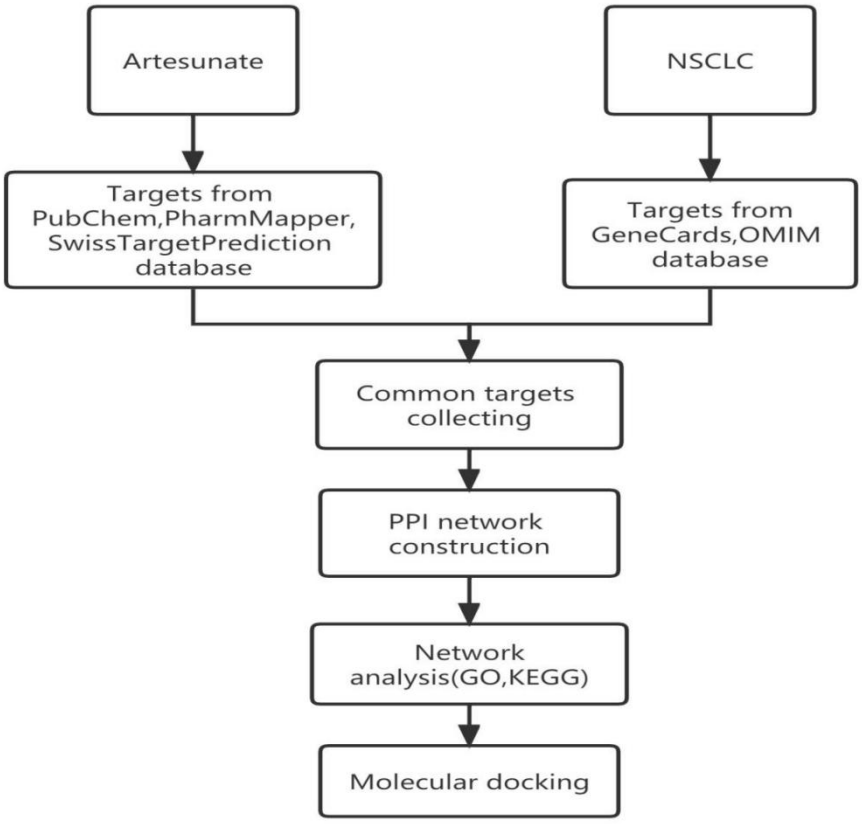

Figure 1: All procedures used in this report

2. Material and methods

2.1. Database and software

PubChem (https://pubchem.ncbi.nlm.nih.gov/), a database of organic small molecule bioactivities; PharmMapper (http://www.lilab-ecust.cn/pharmmapper/), a database of small molecule drug target predictions SwissTargetPrediction (http://www.swisstargetprediction.ch/); human genetic database Genecards (http://www.genecards.org/); human Mendelian genetic database OMMI(https://omim.org/); annotated database of biological information DAVID 6.8 (https://david. ncifcrf.gov/); STRING 11.5, a protein interoperation platform (http://www.string-db.org/); UniProt, a universal protein database

ISSN 2618-1584 Vol. 6, Issue 2: 98-107, DOI: 10.25236/FMSR.2024.060215

(http://www.uniprot.org/uploadlists/); RCSB PDB database (http:/ /www.rcsb.org/); AutoDock 1.5.6 software, PyMOL 2.5.4 software, Venny 2.1.0 online software mapping tool platform (https://bioinfogp.cnb.csic.es/tools/venny/); Cytoscape 3.9.1 software. R4.1.3 software.

2.2. Screening of drug action taargets

To retrieve the two-dimensional chemical structure formula for artesunate, enter its CAS number (88495-63-0) into the Pubchem database and save it in the sdf format. The targets of the two-dimensional chemical structure formula were obtained by importing them into the PharmMapper and SwissTargetPrediction databases. The targets of artesunate were obtained by correcting and unifying the drug target names and de-weighting them in the UniProt database. By entering "non-small cell lung cancer" into Genecards, importing the aforementioned genes into the Vennny2.1 online software mapping tool platform, and taking the intersection genes of artesunate and non-small cell lung cancer, the target genes of artesunate in non-small cell lung cancer were discovered.

2.3. Disease-target-component network construction

In order to create a protein-protein interaction network, the intersecting genes were uploaded to the STRING 11.5 database. The species was set to "Human sapiens," and the confidence level was chosen as high confidence (score value > 0.4). The PPI network data were then imported into Cytoscape. The protein interaction network was visualized using Cytoscape 3.9.1 software after the PPI network data were imported, and the core targets were determined using topology analysis using the NetworkAnalyzer tool.

2.4. GO enrichment analysis of Artesunate-ralated targets and Kyoto Encyclopedia of Genes (KEGG) biological pathway enrichment

The biological information annotation database DAVID 6.8 was used to import the protein targets from the PPI network, and GO biofunctional and KEGG biological pathway enrichment studies were run on the protein targets.

2.5. Molecular docking

Software for pre-docking proteins and small molecule parts is PyMOL, a database of tens of thousands of gene targets is RSCB PDB, and AutoDockTools is software for molecular docking utilizing the semi-flexible method. Candidate targets retrieved from the PPI network are integrated into the RSCB PDB database, and proteins are downloaded in PDB format to improve the reliability of molecular docking results. ChemDraw software is used to process the 3D structures of the components that were obtained from the PubChem database. The structures that had been processed were loaded into the AutoDockTools program to be hydrogenated, charged, and calculated to determine how many rotatable bonds there were. Then, using PyMOL software, ligands and water were taken out of the genes, hydrogen was added, and total charge was computed using AutoDockTools software. We chose the lowest energy pose as the subject of investigation using the clustering feature in AutoDockTools. PyMOL was used to generate precise 3D and 2D structures of small compounds and proteins, and the relevant protein residues and binding links were displayed. It is commonly accepted that when the dock binding free energy is lower than 4 Kcal/mol, the binding ability is stronger.

3. Results

3.1. Artesunate-a target for non-small cell lung cancer

The two-dimensional chemical structure of artesunate is depicted in Figure 2A; import it into the SwissTargetPrediction database, take Probability greater than 0 to get the target of artesunate, and then import it into the PharmMapper database, select "Human Protein Target Only," and take NormFit prediction score greater than 0. After Uniport correction and de-weighting of the projected drug targets from the two databases, 94 candidate targets were found from the SwissTargetPrediction database. We searched the Genecards and OMIM databases, respectively, for "non-small cell lung cancer" to collect all potential targets for the disease. We then checked the Relevance score for the median, and targets bigger than the median were added to obtain more relevant disease targets. Eventually, 3280 disease

ISSN 2618-1584 Vol. 6, Issue 2: 98-107, DOI: 10.25236/FMSR.2024.060215

targets were evaluated after uniform de-duplication. The 65 common target genes were then obtained by importing the artesunate and non-small cell lung cancer targets into Venny 2.1.0, as depicted in Figure 2B.

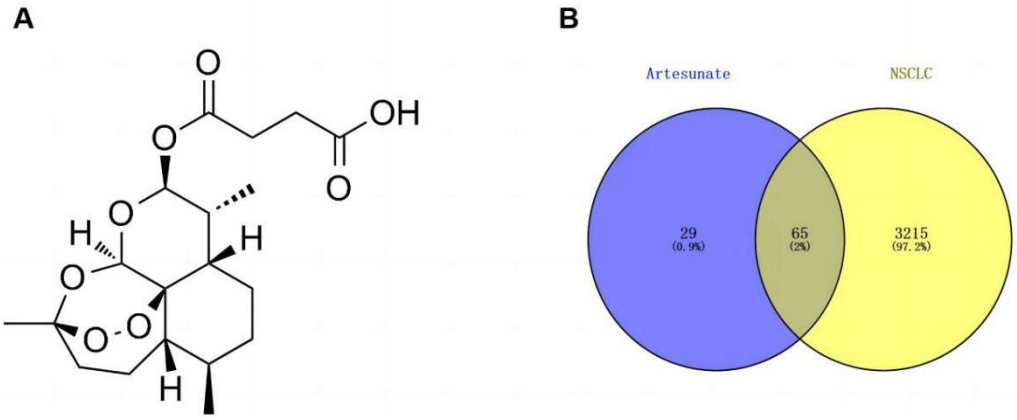

Figure 2: (A) Chemical structure of artesunate. (B) Venn diagram of artesunate targets and NSCLC.

3.2. PPI network interworking analysis

The network relationship data of target interaction was obtained, as shown in Figure 3A, which has 65 nodes and 347 edges. The 65 common target genes were imported into the STRING 11.5 database, the protein type was set as "Homo sapiens," the minimum interaction threshold was 0.4, and the network relationship data of target interaction was obtained. The top 20 targets were plotted in a bar graph using R 4.1.3, as shown in Figure 3B, and CASP3, MMP9, PPARG, MAPK1, PIK3CA, and GSK3B were used for subsequent molecular docking. Topological analysis was also carried out using the NetworkAnalyzer tool in the Cystoscape software. Genes with Degree values greater than the average score were selected as core targets.

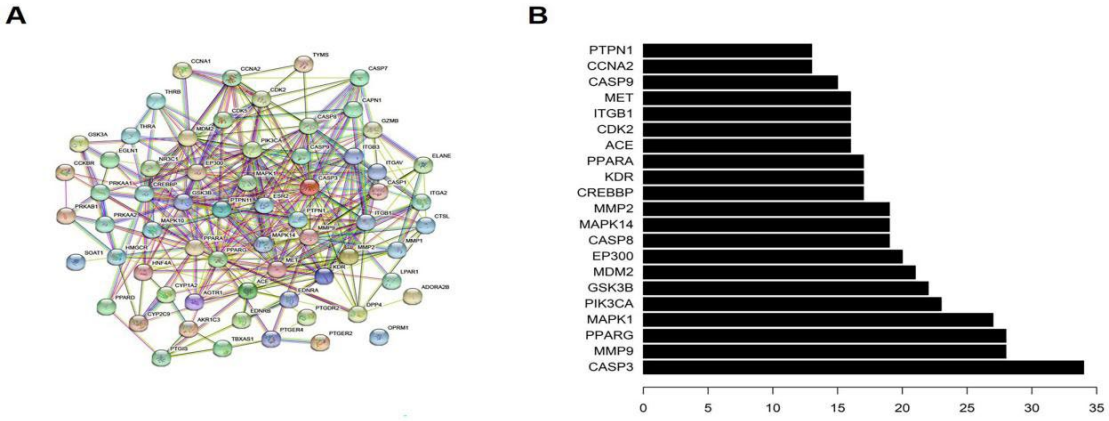

Figure 3: (A) PPI network with the common targets of artesunate and NSCLC. (B) Top 20 common targets of artesunate and NSCLC.

3.3. Building a drug active ingredient-target-disease interraction network

The network diagram showing the relationship between artesunate and non-small cell lung cancer was made using the cytoscap program and is displayed in Figure 4. The green rectangle denotes artesunate, the pink diamond denotes non-small cell lung cancer, and the blue circle denotes the target that both artesunate and non-small cell lung cancer share.

ISSN 2618-1584 Vol. 6, Issue 2: 98-107, DOI: 10.25236/FMSR.2024.060215

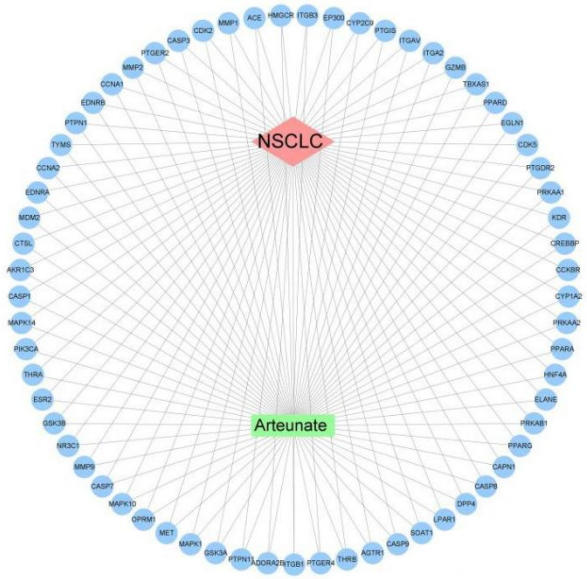

Figure 4: "Artesunate-target-NSCLC" network. Green indicates artesunate; Blue indicates drug-disease intersection proteins; Pink indicates NSCLC.

3.4. Artesunate-non-small cell lung cancer common target GO biofuctional analusis

In order to enrich the biological process (BP), cell component (CC), and molecular function (MF) of GO, the 65 potential common targets of artesunate and non-small cell lung cancer were imported into the DAVID database with the following conditions: PvalueCutoff = 0.05 and QvalueCutoff = 0.05, and the rest of the default settings. The analysis showed that 14 cellular components (CC) were enriched, primarily localizing cytoplasm, nucleus, integrin complex, mitochondria, membrane rafts, and cell cycle protein-dependent protein kinase holoenzyme complex; 46 biological processes (BP) were enriched, mainly regulating and participating in hypoxia response, protein hydrolysis, apoptosis process, signal transduction, cell migration, and negative regulation of RNA polymerase II promoter transcription; As shown in Figure 5, the top 10 functional processes for each component ranked by Pvalue were chosen and plotted in a bubble diagram. The horizontal coordinates show the number of targets, the left side shows BP, CC, and MF, and the color shows the P-value; the smaller the P-value, the more biased the color is, and the larger the P-value, the more biased the color is.

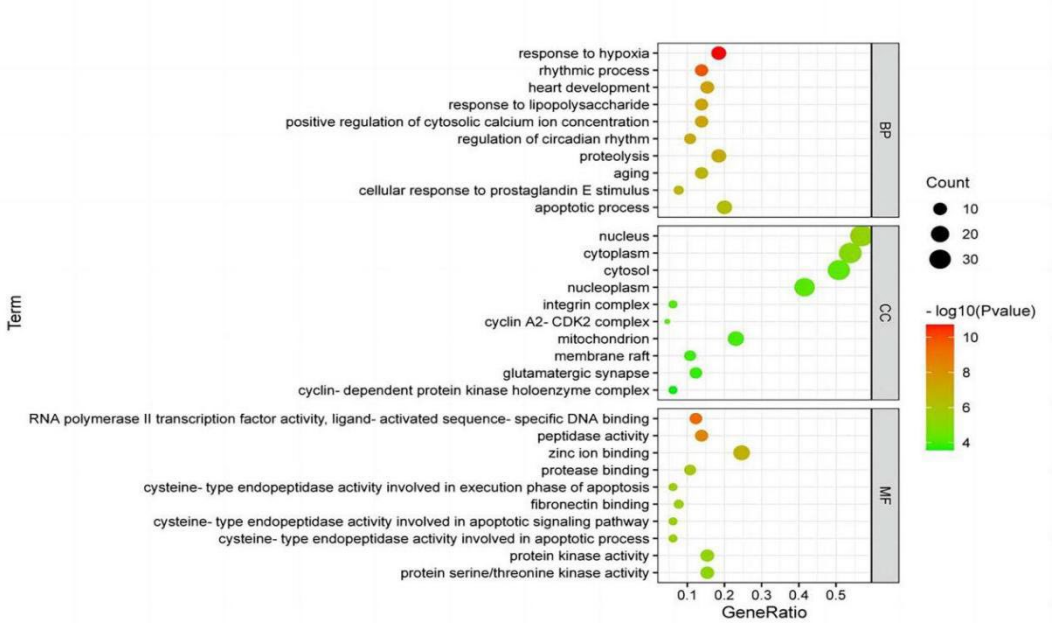

Figure 5: GO enrichment analysis of common targets of artesunate and NSCLC.

ISSN 2618-1584 Vol. 6, Issue 2: 98-107, DOI: 10.25236/FMSR.2024.060215

3.5. KEGG pathway enrichment analysis of common targets of artesunate and non-small cell lung cancer

A total of 81 signaling pathways were enriched when the 65 probable shared targets of artesunate and non-small cell lung cancer were imported into the DAVID database for KEGG pathway enrichment analysis. The KEGG enrichment bubble diagram is displayed in Figure 6, with the horizontal coordinates representing the number of enriched genes, the left side giving the pathway name, and the color indicating the P-value. More red is present when the P-value is lower, and more green is present when the P-value is higher.

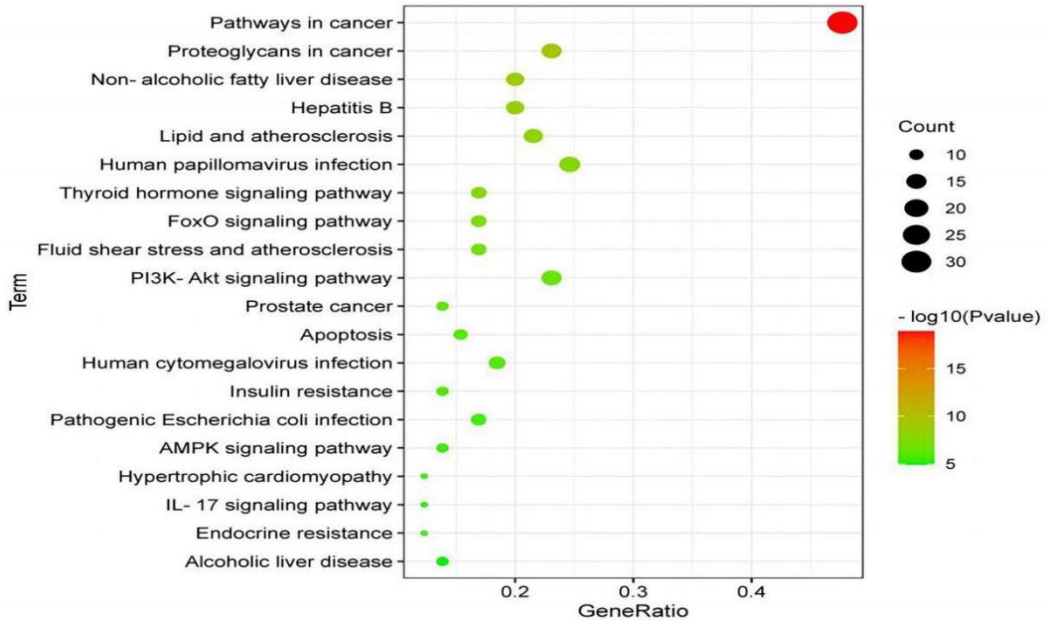

Figure 6: KEGG enrichment of common targets of artesunate and NSCLC.

3.6. Analysis of molecular docking resuts

The PubChem database was used to calculate the molecular weight and 3D structure of ART, and the RCSB PDB database was used to download the associated 3D structure. The necessary ligands and proteins for molecular docking were then created using the AutoDock software. In order to satisfy the low-energy conformation of the ligand structure, the target proteins' crystal structures were decoupled from water molecules, hydrogenated, had their amino acids altered, were energy-optimized, and had their force field parameters changed. Last but not least, ART was used to molecularly dock the six important targets stated in Section 2.2. The Total Score values represent the binding capacities of both bindings; the lower the binding capacities, the more stable the ligand-receptor binding. ART was verified by molecular docking with key targets CASP3, MMP9, PPARG, MAPPK1, PIK3CA, and GSK3B. If the binding energy was smaller, the docking effect was better, and the results showed that all of them had good binding activity, as shown in Table 1 and Figure 7. Finally, the docking results were analyzed and observed using Discovery Studio software.

ISSN 2618-1584 Vol. 6, Issue 2: 98-107, DOI: 10.25236/FMSR.2024.060215

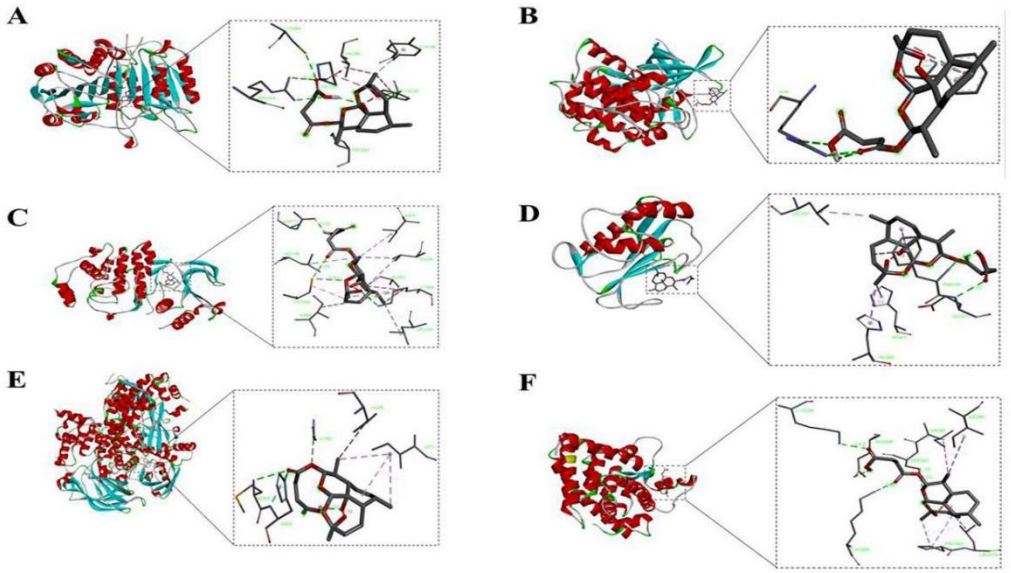

Figure 7: Molecular docking pattern of artesunate with key targets. (A)ART docked with CASP3; (B)ART docked with GSK3B; (C)ART docked with MAPK1; (D)ART docked with MMP9; (E)ART docked with PIK3CA; (F)ART docked with PPARG.

Table 1: Molecular docking results of artesunate and key targets

Chemical Compound	Protein	PDB ID	Total Score	Binding Site
Artesunate	CASP3	1CP3	7.1	A/ARG164, A/PRO201, A/CYS264, B/TYR195, B/TYR197, B/PRO201, B/VAL266
Artesunate	MMP9	1GKD	7.24	A/GLU111, A/LEU187, A/PHE110, A/HIS411, A/HIS405
Artesunate	PPARG	1FM6	10.36	D/LEU270, D/ILE249, D/ILE341, D/LYS244, D/LYS265, D/GLN345, D/SER342
Artesunate	MAPK1	1PME	9.82	A/ILE31, A/VAL39, A/ALA52, A/LYS54, A/ILE84, A/LEU103, A/ASP111, A/LEU156, A/CYS166
Artesunate	PIK3CA	4JPS	7.67	A/MET675, A/HIS676, A/ILE713, A/VAL845, A/GLY842
Artesunate	GSK3B	1J1C	11.2	A/PHE93,A/ARG96

4. Discussion

Advanced non-small cell lung cancer is the most common type of lung cancer with a poor prognosis. Even though personalized therapy and immunotherapy for advanced non-small cell lung cancer have made significant strides recently, only a small percentage of patients have benefited from these treatments, and the eventual development of resistance in the majority of patients necessitates the identification of new targets and the development of novel approaches to combat resistance. Chinese medicine is a significant source of cancer treatment, and experts are beginning to acknowledge its potential in cancer therapy. It is currently one of the most often utilized supplemental medicines to chemotherapy, surgery, and radiotherapy worldwide, particularly in Asia[15]. The Chinese plant Artemisia annua is the source

ISSN 2618-1584 Vol. 6, Issue 2: 98-107, DOI: 10.25236/FMSR.2024.060215

of the semi-synthetic derivative known as artesunate, which has potent antimalarial properties and low adverse effects[16]. Artesunate shows anticancer action in a variety of cancer cells, including lung, ovarian, leukemia, liver, colorectal, and head and neck cancer cells[17-22], according to recent studies. Artesunate affects numerous targets and signaling pathways in cancer and immunological illnesses, according to earlier studies, but a complete understanding of its mechanism of action is still difficult. Network pharmacology offers a good method for modern Chinese medicine research and pharmacological target exploration in this context.

In the current study, the main mechanisms of artesunate's anti-non-small cell lung cancer activity were examined using a mix of network pharmacology and prediction. Cysteine-aspartate protease (CASP3), matrix metalloproteinase 9 (MMP9), peroxisome proliferator-activated receptor (PPARG), phosphatidylinositol kinase-3 catalytic subunit alpha gene (PIK3CA), glycogen synthase kinase 3B (GSK3B) (EIA), EIA-binding protein P300 (EP (CDK2). The MMP family of proteins are collagen hydrolases that break down different protein components of the extracellular matrix, and CASP3 is an essential protease in apoptosis that is activated during apoptosis to alter cell proliferation and apoptosis. The degree of lung cancer cell differentiation and the TNM stage were found to be negatively correlated with MMP-9, and the positive expression rate of MMP-9 was found to be upregulated and correlated with lung cancer metastasis. The positive expression rate of MMP-9 was also found to be significantly higher in patients with survival less than 2 years than in patients with survival greater than or equal to 2 years[23]. The nuclear hormone receptor family, which consists of the three isoforms PPARα, PPARβ/δ, and PPARγ, includes the ligand-activated receptor PPARG. The administration of a PPARG-agonist reduced secondary resistance in gefitinib-resistant lung cancer cells, and it was discovered that PPARG expression was dramatically downregulated in these cells[24]. Additionally, one study discovered that the artemisinin derivative artemether inhibited angiogenesis, which in turn prevented the growth of mouse lung adenocarcinoma cells, and that it increased PPAR expression and decreased NF-B, which prevented the growth and invasion of mouse lung adenocarcinoma transplants[25].

The KEGG pathway enrichment study revealed that the FoxO signaling pathway, PI3K-AKT signaling pathway, AMPK signaling pathway, and other signaling pathways were mostly used by artesunate to treat non-small-cell lung cancer cells. The FoxO signaling pathway is involved in several cellular physiological functions, such as apoptosis, cell cycle control, glucose metabolism, and anti-oxidative stress. The most frequent signaling pathway in the development of cancers originated from humans is PI3K-AKT[26]. This signaling pathway serves a crucial role in preserving the stability of cell metabolism and cell development when it is activated physiologically in the presence of insulin, growth hormones, and cytokines[27]. Through the activation of the PI3K-AKT signaling pathway through oncogenic factors, tumor cells play a significant role in the regulation of cell proliferation, apoptosis, angiogenesis, and drug sensitivity under pathological conditions. This process enhances the activity of nutrient transporters and metabolism and rewires cell metabolism to support abnormal cell growth and metabolic demand [28, 29].

5. Conclusion

In conclusion, this study discovered that artesunate, based on network pharmacology, has a multi-target and multi-pathway action against non-small cell lung cancer. More in vivo and ex vivo research is required, however, to fully understand the anti-non-small cell lung cancer effects and associated processes of artesunate. This will help to support the use of Chinese medicine in the prevention and treatment of lung cancer.

Acknowledgements

This paper is supported by Science and Technology Department of Guizhou Province under grant (No.[2020]4Y156) and 2021 Graduate Research Fund Projects under grant (No.ZYK146)

References

[1] Abrishami Kia Z, Sadati Bizaki ST, Asaádi Ghareh Tapeh E, et al. Managing MMP-2, MMP-9, VEGFR-2, TGFβ-1, and TIMP-1 in NNK-induced lung carcinoma by nonchemical interventions in female rats. Toxicol Rep, 2022, 9:1261-1267.

[2] Xia C, Dong X, Li H, et al. Cancer statistics in China and United States, 2022: profiles, trends, and

ISSN 2618-1584 Vol. 6, Issue 2: 98-107, DOI: 10.25236/FMSR.2024.060215

determinants. Chinese medical journal, 2022, 135(5):584-590.
[3] Duma N, Santana-Davila R, Molina J. Non-Small Cell Lung Cancer: Epidemiology, Screening, Diagnosis, and Treatment. Mayo Clinic proceedings, 2019, 94(8):1623-1640.
[4] Herbst R, Morgensztern D, Boshoff C. The biology and management of non-small cell lung cancer. Nature, 2018, 553(7689):446-454.
[5] Denis F, Basch E, Septans A, et al. Two-Year Survival Comparing Web-Based Symptom Monitoring vs Routine Surveillance Following Treatment for Lung Cancer. JAMA, 2019, 321(3):306-307.
[6] Zhao F, Vakhrusheva O, Markowitsch S, et al. Artesunate Impairs Growth in Cisplatin-Resistant Bladder Cancer Cells by Cell Cycle Arrest, Apoptosis and Autophagy Induction. Cells, 2020, 9(12).
[7] Greenshields A, Fernando W, Hoskin D. The anti-malarial drug artesunate causes cell cycle arrest and apoptosis of triple-negative MDA-MB-468 and HER2-enriched SK-BR-3 breast cancer cells. Experimental and molecular pathology, 2019, 107:10-22.
[8] Cao D, Chen D, Xia J, et al. Artesunate promoted anti-tumor immunity and overcame EGFR-TKI resistance in non-small-cell lung cancer by enhancing oncogenic TAZ degradation. Biomed Pharmacother, 2022, 155:113705.
[9] Geng B, Zhu Y, Yuan Y, et al. Artesunate Suppresses Choroidal Melanoma Vasculogenic Mimicry Formation and Angiogenesis the Wnt/CaMKII Signaling Axis. Front Oncol, 2021, 11:714646.
[10] Meng Q, Zhang X, Zhang Z, et al. Therapeutic potential of artesunate in experimental autoimmune myasthenia gravis by upregulated T regulatory cells and regulation of Th1/Th2 cytokines. Die Pharmazie, 2018, 73(9):526-532.
[11] Su T, Li F, Guan J, et al. Artemisinin and its derivatives prevent Helicobacter pylori-induced gastric carcinogenesis via inhibition of NF-κB signaling. Phytomedicine : international journal of phytotherapy and phytopharmacology, 2019, 63:152968.
[12] Xu Z, Liu X, Zhuang D. Artesunate inhibits proliferation, migration, and invasion of thyroid cancer cells by regulating the PI3K/AKT/FKHR pathway. Biochem Cell Biol. 2022, 100(1):85-92.
[13] Li W, Ma G, Deng Y, et al. Artesunate exhibits synergistic anti-cancer effects with cisplatin on lung cancer A549 cells by inhibiting MAPK pathway. Gene, 2021, 766:145134.
[14] Jain B, Raj U, Varadwaj P. Drug Target Interplay: A Network-based Analysis of Human Diseases and the Drug Targets. Current topics in medicinal chemistry, 2018, 18(13):1053-1061.
[15] M ohebbati R, Paseban M, Soukhtanloo M,et al. Effects of standardized Zataria multiflora extract and its major ingredient, Carvacrol, on Adriamycin-induced hepatotoxicity in rat. Biomed J, 2018, 41(6):340-347.
[16] Zhang J, Li Y, Wan J, et al. Artesunate: A review of its therapeutic insights in respiratory diseases. Phytomedicine : international journal of phytotherapy and phytopharmacology, 2022, 104:154259.
[17] Zhang W, Ning N, Huang J. Artesunate Suppresses the Growth of Lung Cancer Cells by Downregulating the AKT/Survivin Signaling Pathway. BioMed research international, 2022, 2022:9170053.
[18] Chen X, Zhang X, Zhang G, Gao Y. Artesunate promotes Th1 differentiation from CD4+ T cells to enhance cell apoptosis in ovarian cancer via miR-142. Braz J Med Biol Res. 2019, 52(5):e7992.
[19] Chen S, Gan S, Han L, et al. Artesunate induces apoptosis and inhibits the proliferation, stemness, and tumorigenesis of leukemia. Annals of translational medicine, 2020, 8(12):767.
[20] Yao X, Zhao C, Yin H, et al. Synergistic antitumor activity of sorafenib and artesunate in hepatocellular carcinoma cells. Acta pharmacologica Sinica, 2020, 41(12):1609-1620.
[21] Jiang F, Zhou J, Zhang D, et al. Artesunate induces apoptosis and autophagy in HCT116 colon cancer cells, and autophagy inhibition enhances the artesunate-induced apoptosis. International journal of molecular medicine, 2018, 42(3):1295-1304.
[22] Xiao Q, Yang L, Hu H, et al. Artesunate targets oral tongue squamous cell carcinoma via mitochondrial dysfunction-dependent oxidative damage and Akt/AMPK/mTOR inhibition. J Bioenerg Biomembr, 2020, 52(2):113-121.
[23] Abrishami Kia Z, Sadati Bizaki S, Asaádi Ghareh Tapeh E, et al. Managing MMP-2, MMP-9, VEGFR-2, TGFβ-1, and TIMP-1 in NNK-induced lung carcinoma by nonchemical interventions in female rats. Toxicology reports,2022, 9:1261-1267.
[24] Ni J, Zhou L, Ding L, et al. Efatutazone and T0901317 exert synergistically therapeutic effects in acquired gefitinib-resistant lung adenocarcinoma cells. Cancer Med-Us, 2018, 7(5):1955-1966.
[25] Chen J, Huang X, Tao C, et al. Artemether Attenuates the Progression of Non-small Cell Lung Cancer by Inducing Apoptosis, Cell Cycle Arrest and Promoting Cellular Senescence. Biological & pharmaceutical bulletin, 2019, 42(10):1720-1725.
[26] Yu L, Wei J, Liu P. Attacking the PI3K/Akt/mTOR signaling pathway for targeted therapeutic treatment in human cancer. Semin Cancer Biol, 2022, 85:69-94.
[27] Hoxhaj G, Manning BD. The PI3K-AKT network at the interface of oncogenic signalling and cancer

ISSN 2618-1584 Vol. 6, Issue 2: 98-107, DOI: 10.25236/FMSR.2024.060215

metabolism. Nature Reviews Cancer, 2020, 20(2):74-88.
[28] Zhang L, Zheng Y, Zeng L, et al. 3-Epipachysamine B suppresses proliferation and induces apoptosis of breast cancer cell via PI3K/AKT/mTOR signaling pathway. Life Sciences, 2021, 285:119995.
[29] Hu F, He Z, Sun C, et al. Knockdown of GRHL2 inhibited proliferation and induced apoptosis of colorectal cancer by suppressing the PI3K/Akt pathway. Gene, 2019, 700.